



Assessment of an ensemble seasonal streamflow forecasting system for Australia

James C. Bennett^{1,2}, Quan J. Wang³, David E. Robertson¹, Andrew Schepen⁴, Ming Li⁵, Kelvin Michael²

5 ¹CSIRO Land & Water, Clayton, Victoria, Australia

²Institute for Marine and Antarctic Studies, University of Tasmania, Hobart, Tasmania, Australia

³Department of Infrastructure Engineering, The University of Melbourne, Parkville, Victoria, Australia

⁴CSIRO Land & Water, Dutton Park, Queensland, Australia

⁵CSIRO Data61, Floreat, Western Australia, Australia

10 *Correspondence to:* James C. Bennett (james.bennett@csiro.au)

Abstract. Despite an increasing availability of skillful long-range streamflow forecasts, many water agencies still rely on simple resampled historical inflow sequences (stochastic scenarios) to plan operations over the coming year. We assess a recently developed forecasting system called *forecast guided stochastic scenarios* (FoGSS) as a skillful alternative to standard stochastic scenarios for the Australian continent. FoGSS uses climate forecasts from a coupled ocean-land-atmosphere prediction system, post-processed with the method of calibration, bridging and merging. Ensemble rainfall forecasts force a monthly rainfall-runoff model, while a staged hydrological error model quantifies and propagates hydrological forecast uncertainty through forecast lead times. FoGSS is able to generate ensemble streamflow forecasts in the form of monthly time series to a 12-month forecast horizon.

FoGSS is tested on 63 Australian catchments that cover a wide range of climates, including 21 ephemeral rivers. In all perennial and many ephemeral catchments, FoGSS provides an effective alternative to resampled historical inflow sequences. FoGSS generally produces skillful forecasts at shorter lead times (<4 months), and transits to climatology-like forecasts at longer lead times. Forecasts are generally reliable and unbiased. However, FoGSS does not perform well in very dry catchments (catchments that in experience zero flows more than half the time in some months), sometimes producing strongly negative forecast skill and poor reliability. We attempt to improve forecasts through the use of i) ESP rainfall forcings, ii) different rainfall-runoff models, and iii) a Bayesian prior to encourage the error model to return climatology forecasts in months when the rainfall-runoff model performs poorly. Of these, only the use of the prior offered clear benefits in very dry catchments, where it moderated strongly negative forecast skill and reduced bias in some instances. However, the prior did not remedy poor reliability in very dry catchments.

Overall, FoGSS is an attractive alternative to historical inflow sequences in all but the driest catchments. We discuss ways in which forecast reliability in very dry catchments could be improved in future work.

Keywords. Seasonal streamflow forecasting; ensemble prediction; CGCM; hydrological uncertainty; error modelling



1 Introduction

Recent years have seen a proliferation of experimental long-range ensemble streamflow forecasting systems (examples from this issue: Meißner et al., 2017; Beckers et al., 2016; Candogan Yossef et al., 2016; Bell et al., 2017; Greuell et al., 2016), and, to a lesser extent, the operationalization of these systems as forecasting services that are available to water agencies and the public. In Australia, the Bureau of Meteorology runs a freely available seasonal streamflow forecasting service that predicts total streamflow for the coming 3 months at more than 200 sites across Australia (www.bom.gov.au/water/ssf/). While the Bureau's service has been well received by Australian water agencies, a number of agencies still rely primarily on resampled historical inflow sequences, not forecasts, to plan operations for the coming year. Resampled historical inflow sequences (termed stochastic scenarios in this paper) have some appeal for water agencies: they are unbiased, they are available as time series, they are easy to generate to long time horizons, and, presuming a long observation record is available from which to sample, the ensemble of inflows is inherently statistically reliable (either taken at individual months or when individual ensemble members are summed, e.g., to produce an ensemble of 6-month total inflow). The Bureau's service is based on a statistical method, the Bayesian joint probability (BJP) modelling approach (Wang and Robertson, 2011), which uses information from current streamflow conditions and climate indices to produce skillful streamflow forecasts. The BJP is able to produce skillful, unbiased forecasts with highly reliable ensembles, and can be used to generate monthly volume forecasts to short (e.g. 3-month) forecast horizons (Zhao et al., 2016). But the BJP is not well suited to generating time series forecasts to long (12-month) time horizons. Other seasonal forecasting systems generally have some combination of short-comings with respect to stochastic scenarios: they may not produce reliable ensembles (e.g., Crochemore et al., 2016); the ensembles may be biased with respect to climatology; and/or the forecasts may be less skillful than climatology for certain months or lead times. Any of these can be a serious barrier to their use by water agencies to plan future operations.

Of course, stochastic scenarios have a major short-coming of their own: they take no account of information from current catchment and climate conditions, and thus offer no skill to water agencies. To attempt to combine the practical advantages of stochastic scenarios with useful information contained in forecasts, we recently proposed a new streamflow forecasting system called *forecast guided stochastic scenarios*, or FoGSS. FoGSS uses statistically post-processed climate forecasts from a coupled climate forecasting system to force a monthly rainfall-runoff model, together with a hydrological error model that updates forecasts, corrects biases, and propagates forecast uncertainty through the lead times. FoGSS is designed to offer time series forecasts to long time horizons (12 months). As forecast skill declines with lead time, FoGSS is designed to return forecasts that converge to climatology. Each ensemble member in the forecast is a realistic 12-month hydrograph at a monthly time step. In a previous paper (Bennett et al., 2016), we described the theoretical underpinnings of FoGSS and showed that it performed well for two high-rainfall Australian catchments, producing skillful and reliable ensemble forecasts. We noted that the viability of FoGSS as a continent-wide forecasting system remained to be tested. In particular, FoGSS needs to be tested for ephemeral rivers, which are an important source of water (e.g. for agriculture) in many Australian regions.

The aim of this paper is to test FoGSS on a wide range of Australian catchments that encompass different climatic and hydrologic conditions. We then vary components of the system - rainfall forcings, rainfall-runoff modelling, and the hydrological error model - to assess to what extent, if any, forecasts can be improved. The paper is structured as follows. We give an overview of the FoGSS model in Section 2, and describe our experiments to



vary elements of FoGSS in Section 3. We present and discuss our results in Section 4, and we summarise and conclude our findings in Section 5.

2 The FoGSS Model

A schematic of the FoGSS model is shown in Figure 1.

5 2.1 Ensemble rainfall forecasts

Rainfall and sea-surface temperature (SST) predictions are taken from the POAMA M2.4 seasonal climate forecasting system (Marshall et al., 2014; Hudson et al., 2013). POAMA reforecasts are available as a 33-member ensemble; comprised of 11 members each from three variants of the model. We use forecasts issued at the start of each calendar month (12 forecasts a year) from 1982–2010. These forecasts are then post-processed with the method of calibration, bridging and merging (CBaM; Schepen and Wang, 2014; Schepen et al., 2014). While POAMA produces skillful rainfall forecasts in some months and seasons in parts of Australia, it suffers from deficiencies common to many dynamical climate forecasting models: forecasts are often biased at the scale of catchments; forecast ensembles tend to be overconfident; and forecasts may be substantially less skillful than climatology in certain months and seasons (Schepen et al., 2016).

15 We have shown elsewhere that it is only possible to correct all these deficiencies by calibration, rather than applying a simple bias-correction (Zhao et al., 2017). Accordingly, POAMA rainfall reforecasts are calibrated to each catchment with the BJP, which uses Bayesian inference, data transformation (Wang et al., 2012b) and a bivariate normal distribution to establish a statistical relationship between observations and rainfall forecasts and for each month and lead time. The statistical relationship is then used to generate forecasts. This approach is highly effective at removing bias, correcting ensemble spread, and ensuring forecasts are ‘coherent’ - that is, never less skillful than climatology forecasts (Hawthorne et al., 2013; Peng et al., 2014; Schepen et al., 2016). To maximise the skill of rainfall forecasts, we use ‘bridging’ to build statistical relationships between POAMA SST forecasts and catchment rainfall, again with the BJP. Bridging also allows us to generate forecasts to 12-month forecast horizons: POAMA produces forecasts only to 9 months in advance; we use bridging to establish relationships between 9-month SST forecasts and 10-, 11- and 12-month forecast horizons. To merge the calibration and bridging forecasts we use Bayesian model averaging (Wang et al., 2012a) to produce a forecast ensemble of 1000 members. Finally, realistic temporal patterns are instilled in each forecast ensemble member with the Schaake shuffle (Clark et al., 2004).

2.2 Hydrological error model

30 Precipitation forecasts are used to force an initialised monthly rainfall-runoff model. In the original conception of FoGSS, we used the Wapaba model (Wang et al., 2011). In this study, we test two other rainfall-runoff models, and we describe all three rainfall-runoff models in Section 3.4. Forcing a hydrological model with ensemble precipitation forecasts results in ensemble streamflow forecasts that are overconfident, as uncertainty in the hydrological model is not incorporated into the forecast. In addition, hydrological models, even when optimised, are usually subject to errors and bias. To address these issues, FoGSS employs a 3-stage error model. The model is broken into stages to avoid undesirable interaction between parameters when they are optimized, with each stage described separately (sections 2.2.1, 2.2.2 and 2.2.3).



Parameters for each stage are estimated sequentially using maximum likelihood estimation (MLE). We give only a brief overview of the estimation procedure here, and refer the reader to Bennett et al. (2016) for a detailed description, including full likelihood equations. Stage 1 parameters are estimated and fixed, followed by Stage 2 and then Stage 3. We employ data transformation (Stage 1) so that residuals are normally distributed and heteroscedastic. For ephemeral rivers, this is not enough to satisfy the requirement of MLE for continuously distributed data. To handle zero values, we treat observations of zero as censored values in the likelihood, a technique established previously (Li et al., 2013).

A notable aspect of the estimation of hydrological and error model parameters is that we take no account of lead time in the parameter estimation. That is, parameters are estimated only from rainfall-runoff simulations (forced by observed rainfall and potential evaporation) and observed streamflow, as with a conventional rainfall-runoff model calibration. This is a key difference with approaches that post-process streamflow forecasts separately at each lead time (e.g. Yuan, 2016), as it means that each FoGSS time series forecast is a continuous hydrograph that can be summed to produce reliable ensembles of, e.g., seasonal inflow totals. However, the FoGSS error model will not correct problems associated with ensemble rainfall forecasts (e.g. overconfident ensembles). FoGSS requires ensemble rainfall forecasts that are unbiased and reliable in order to produce unbiased and reliable streamflow forecasts.

2.2.1 Stage 1: data transformation and hydrological modelling

It is widely recognised that errors from hydrological models are neither normally distributed nor homoscedastic (e.g., Schaefli et al., 2007; Smith et al., 2015), and therefore difficult to model using conventional statistical methods. One method for addressing these problems is to use data transformation. We use the log-sinh transformation (Wang et al., 2012b), which has proven highly effective for normalising hydrological data and homogenising variance (e.g. Del Giudice et al., 2013). The log-sinh transformation is given by:

$$z = TF(q) = \frac{1}{b} \log(\sinh(a + bq)) \quad (1)$$

where q is streamflow a and b are parameters. The inverse transformation (back transformation) is given by

$$q = TF^{-1}(z) = \max\left(\frac{1}{b}(\operatorname{argsinh}(e^{bz}) - a), 0\right), \quad (2)$$

where z is any streamflow in the transformed domain. For clarity, we will refer to the domain in which q exists as the original domain to differentiate it from the transform domain of z .

The parameters in Eq. (1) are estimated from observed streamflow. Once transformation parameters are obtained, hydrological model parameters (Section 3.4) are estimated with MLE.

2.2.2 Stage 2: bias-correction

Transformed streamflow is bias-corrected at each time t by

$$z_2(t) = d(i)z_1(t) + \mu(i), \quad (3)$$

where z_1 is the raw streamflow forecast after transformation with Eq. 1, and $d(i)$ and $\mu(i)$ are parameters that vary by month,

$$i = 1, 2, \dots, 12 = \text{month}(t), \quad (4)$$



Although Eq. (3) takes is a simple linear regression, because it is applied to transformed flows it is able to correct highly non-linear biases in the original domain. An important feature of Eq. (3) is that the d parameter can go to zero. That is, in months where the hydrological simulation performs poorly, the error model can return $z_2 \approx \mu$, a constant akin to a climatology. As we shall see, this is a particularly important property in ephemeral catchments.

We limit d to the range $0 \leq d \leq 2$. Values less than zero imply a negative correlation between simulations and observations, and in these cases it is more sensible to ignore the simulation (i.e., to allow $d=0$). The upper limit of 2 is arbitrary, and is imposed to avoid unrealistically large corrections that could result in overfitting of the bias-correction.

2.2.3 Stage 3: Autoregressive model and stochastic updating

FoGSS applies a restricted first-order autoregressive (AR1) model (Li et al., 2015) to improve accuracy of forecasts and to propagate hydrological uncertainty through the forecast lead times. The AR1 model is applied to transformed, bias-corrected flows by:

$$z_3(t) = z_2(t) + \rho(i)(z_o(t-1) - z_2(t-1)), \quad (5)$$

where z_o is transformed observed streamflow and $\rho(i)$ is the autoregression parameter, varied by calendar month. Because the AR1 model is applied in the transform domain, the magnitude of the correction can be greatly amplified in the original domain if it is applied to a rising hydrograph, leading to unrealistically large streamflows. To avoid this type of overcorrection, we apply the restriction proposed by Li et al. (2015). This restriction corrects the forecast by whichever is smaller: the error in the original domain at $t-1$, or the correction proposed by Eq. (5). As with the previous stages, when estimating Stage 3 parameters with MLE we assume errors, ε , are normally distributed:

$$\begin{aligned} z_o(t) &= z_3(t) + \varepsilon(i) \\ \varepsilon(i) &\sim N(0, \sigma^2(i)) \end{aligned} \quad (6)$$

where $\sigma^2(i)$ is the variance of ε at each calendar month.

Finally, hydrological uncertainty is propagated with stochastic updating. At the first lead time, $l=0$, this is straightforward: we have an observation available when the forecast is issued, and hence we can apply Eq. (5) directly, and then add noise according to Eq. (6) to produce a forecast value z_f . At longer lead times $l=1, \dots, 11$ we do not have observations available with which to update the forecast. Instead, we substitute the forecast value, z_f , for the observation, z_o , in Eq. (5), and forecasts are generated by:

$$\begin{aligned} z_f(t+l) &= z_2(t+l) + \rho(i)(z_f(t+l-1) - z_2(t+l-1)) + \varepsilon(i) \quad | l=1, \dots, 11 \\ \varepsilon(i) &\sim N(0, \sigma^2(i)) \end{aligned} \quad (7)$$

In this way hydrological uncertainty grows through the forecast, as expected (i.e., forecasts become less certain at longer lead times). As with Eq. (5), the restriction described above is applied to Eq. (7).



3. Experiments

3.1 General setup

3.1.1 Forecast cross-validation

5 Thorough validation of forecast systems requires a large population of reforecasts to allow testing over a variety of conditions and to be able to calculate robust probabilistic verification scores. Unfortunately, reforecasts are often limited in number, in our case because of the availability of POAMA reforecasts (see Section 2.1). Rigorous cross-validation is a vital element of robust forecast validation. We use the following scheme:

1. The post-processing of rainfall forecasts is cross-validated using leave-3-years out cross-validation
2. Hydrological and error models are cross-validated using leave-5-years out cross-validation.

10 A more stringent cross-validation is required for hydrological models because catchment memory is more persistent than memory in seasonal weather patterns or SST (i.e., current catchment conditions can influence streamflow over the next 2 or more years in some catchments).

To estimate parameters and to generate forecasts, the hydrological model is initialised by running it from January, 1970.

3.1.2 Verification scores

15 In accordance with most studies of ensemble forecasting systems, we are chiefly concerned with two aspects of forecast performance: forecast skill and forecast reliability. To measure forecast skill, we use the well-known continuous ranked probability score (CRPS; see, e.g., Gneiting and Katzfuss, 2014). Skill is measured against “climatology”, or historical frequency, of streamflow. Forecast skill is given by the continuous ranked probability skill score (CRPSS):

$$20 \quad CRPSS = \frac{CRPS_{Ref} - CRPS_F}{CRPS_{Ref}} \times 100\%, \quad (8)$$

where $CRPS_F$ and $CRPS_{Ref}$ are CRPS values for FoGSS and cross-validated climatology forecasts, respectively. To generate climatology reference forecasts, a log-sinh transformed (Eq. 1) normal distribution is fitted to the observed streamflow data for each month. 1000 samples are drawn from the transformed normal distribution to generate a climatology. Climatology is generated using observed data for the period 1982-2009, applying the same leave-5-years-out cross-validation procedure as described for the hydrological modelling (Section 3.2). Zero values are handled through data censoring, as described by Wang and Robertson (2011); that is, the climatology reference forecasts correctly replicate the incidence of zero flows. In some very dry catchments, some months recorded only one or no non-zero flows for the period 1982-2009. In these cases it is not possible to fit a distribution. Here, we take a pragmatic approach: we simply assign a reference forecast of zero.

25 As noted in the introduction, a key attribute of stochastic scenarios is that they are inherently unbiased and thus can be used directly in planning models by water agencies. To be a viable alternative to stochastic scenarios, FoGSS forecasts should be unbiased. Absolute relative bias of forecasts is calculated at each lead time, l , by

$$30 \quad Bias(l) = \left| \frac{\overline{q_f(l)} - \overline{q_o}}{\overline{q_o}} \times 100\% \right|, \quad (9)$$



where $\overline{q_f(l)}$ is the mean of all ensemble forecasts at each lead time. (For brevity, absolute relative bias is simply referred to as bias throughout the paper.)

The statistical reliability of ensemble forecasts is assessed with probability integral transform (PIT) - uniform probability plots (shortened to *PIT plots*). Given the cumulative distribution function (CDF) of a forecast at time t , C_t , the PIT of the accompanying observed value, $q_o(t)$, is given by:

$$\pi_t = C_t(q_o(t)). \quad (10)$$

When a set of forecasts is reliable, the set of π_t values is uniformly distributed between 0 and 1, and the resulting PIT plot will follow the diagonal one-to-one line. In catchments with zero values, the CDF in Equation (10) will not be continuous (and therefore cannot be expected to follow a uniform distribution). In these catchments, if $q_o(t) = 0$ we generate a *pseudo-PIT* value π_t randomly sampled from a uniform distribution in the range $[0, C_t(0)]$.

To compare reliability for many catchments we summarise information from PIT plots with the alpha index (Renard et al., 2010)

$$\alpha = 1 - \frac{2}{n} \sum_{i=1}^n \left| \pi_i^* - \frac{i}{n+1} \right|, \quad (11)$$

where π_i^* is the sorted π_t in increasing order, and n the number of forecasts. The alpha index essentially reflects the divergence of PIT values from the 1-1 line in PIT plots.

3.1.1 Catchments and data

We assess FoGSS forecasts on 63 Australian catchments ranging in size from <100 km² to >200,000 km² (Appendix A). Catchments are distributed across the continent, encompassing temperate, desert, subtropical and tropical climates. Rainfall and potential evaporation data are taken from the gridded AWAP dataset, which interpolates gauged observations (Australian Water Availability Project, <http://www.bom.gov.au/jsp/awap>). Streamflow data are mainly from gauges, but we have also included several ‘inflow sites’, which are not directly gauged. The inflow site records give total inflow to storages, and are calculated from a combination of streamflow gauge records, storage levels, and discharge from storages. We include these sites because they are of good quality, and often of central importance to water agencies. All streamflow data records have been supplied and checked for quality by the Bureau of Meteorology.

Of the catchments we assess, one third – 21 catchments – are ephemeral rivers (defined as having zero flows in > 4% of their records), occurring in both temperate and tropical climates. As ephemeral rivers tend to be very difficult to predict – they can exhibit strongly non-linear responses of rainfall to runoff; they often experience highly sporadic rainfall – we pay particular attention to these catchments. To illustrate different aspects of the performance of FoGSS, we choose a subset of six catchments (Table 1). The streamflow characteristics of these rivers is shown in Figure 2 and each is briefly described:

- **Fitzroy River** (Western Australia): Has a large catchment area, and ceases to flow only occasionally (Figure 2). Like all northern, tropical regions in Australia, the Fitzroy receives most rainfall in the monsoon period Nov-Mar, and very little rainfall at other times of the year.



-
- **Ranken River** (Northern Territory): An extremely dry catchment that ceases to flow for long periods, flowing regularly only in Mar. Can record zero flows at any time of year, and is usually dry from Apr-Dec. Over the period 1982-2009, the river never flowed in September.
 - **Herbert River** (Queensland): Perennial River that receives the bulk of its rainfall in the northern monsoon period (Nov-Mar).
 - **Lake Eppalock inflows** (Victoria): Lake Eppalock receives inflow from the temperate and seasonally ephemeral Campaspe River, largely in the period Jul-Nov. This is a high-quality inflow series synthesised from stream gauge and storage level records. Often receives zero inflow in late summer to early autumn (Jan-Apr).
 - **Goobarragandra River** (New South Wales): Perennial River that receives most rainfall in the winter and spring (Jun-Nov). This catchment generally exhibits strong catchment memory.
 - **Ringarooma River** (Tasmania): alpine, temperate river that receives regular, winter dominant rainfall (Jun-Aug), but has little catchment memory.

3.2 Base case: continent-wide performance assessment of FoGSS

To establish whether FoGSS is a system capable of being deployed across the Australian continent, we test FoGSS as it was described by Bennett et al. (2016): that is, as described in Section 2, using the Wapaba rainfall-runoff model. This constitutes the base case, against which the following variations will be tested. The performance of the base case is assessed by skill, reliability and bias (Section 3.1.2).

3.3 Experiment 1: Contribution of rainfall forecasts to skill

To assess the contribution of rainfall forecasts to overall streamflow forecast skill, we compare our base case to ESP-like forecasts (extended streamflow predictions). Traditional ESP methods use resampled historical rainfall to force an initialised hydrological model (Day, 1985). An ensemble of historical rainfall forcings is reliable and unbiased but completely uninformative, so any forecast skill remaining will be due to catchment memory (Wood and Lettenmaier, 2008). We use a similar approach, except that we also apply the FoGSS hydrological error model. By comparing streamflow forecasts generated with ESP-like historical rainfall forcings to those generated with the full FoGSS system, we can determine the relative contribution of post-processed POAMA forecasts to overall forecast skill. Rainfall observations are resampled from the period 1982-2009, using a leave-4-years-out cross-validation scheme. (The leave-4-years-out scheme was chosen in part for computational convenience: it results in a forcing ensemble of 25 members, which divides evenly into 1000, the size of the FoGSS ensemble.) To produce a 1000-member ensemble, we run each historical rainfall sequence through the FoGSS hydrological and error models forty times, using a different random seed at the start of each run. To keep the distinction clear, we refer to the post-processed POAMA forcings as *forecast rainfall* to distinguish them from the ESP-like *historical rainfall* forcings.

3.4 Experiment 2: hydrological modelling

As already noted, the original conception of FoGSS made use of the Wapaba rainfall-runoff model (Wang et al., 2011). Wapaba is a five-parameter conceptual hydrological model based on the Budyko curve, which casts the water balance as a competition between available water and available energy. Its parameters and a schematic of



its structure are given in Appendix B. Wapaba performed well in a study that compared it to other rainfall-runoff models for simulating 331 (largely) perennial Australian rivers (Wang et al., 2011). However, as we will see, Wapaba's performance is more equivocal for forecasts for ephemeral rivers.

To test whether performance can be improved using alternative rainfall-runoff models, we substitute two alternative monthly rainfall-runoff models, ABCD and GR2M, into the FoGSS system. ABCD (Alley, 1984; Thomas, 1981) is a four-parameter monthly water balance model and GR2M (Mouelhi et al., 2006) is a simpler model with only two parameters. Parameters and structures of the two models are shown in Appendix B. In general, ABCD and Wapaba are more similar to each other than to GR2M. ABCD and Wapaba each have two parameters to control the apportionment of water between the surface water store and groundwater/direct runoff, while GR2M simply relies on an empirical equation for this apportionment. All three models have two conceptual soil moisture stores, but they function slightly differently in each case. The surface stores in ABCD and Wapaba can lose water only to evaporation or when the storage spills. GR2M's production store loses water to evaporation and spill, but also drains to the routing store at a non-linear rate in relation to the level of the production store. ABCD and Wapaba both have groundwater stores of unlimited capacity and both have parameters to control the (linear) rate of discharge from the groundwater store. GR2M has a finite (and fixed) groundwater storage capacity, and uses a fixed (non-linear) relationship to govern discharge from its routing store. In both Wapaba and ABCD, catchment losses are entirely controlled by evaporation. In GR2M water can be lost to, or gained from, an unlimited conceptual groundwater store outside the catchment. Wapaba and ABCD differ in the way that they apportion water between soil moisture stores and groundwater and direct runoff, and have different methods to calculate actual evaporation from the surface store.

Rainfall-runoff model parameters are estimated using maximum likelihood. Parameters of the subsequent stages of the error model (stages 2 and 3) are then estimated, as described in Section 2.2. That is, only the rainfall-runoff models and Stage 2 and Stage 3 error model parameters change in this experiment: all other elements of FoGSS remain the same.

25 3.5 Experiment 3: encouraging the error model to return climatology forecasts

As we shall see, the FoGSS system is outperformed by climatology in some very dry catchments. FoGSS forecasts need not necessarily outperform climatology to function as a viable alternative to stochastic scenarios, but they do need to be at least similarly skillful to climatology (we term this *neutrally skillful*). One way to achieve this is to encourage the error model to return climatology forecasts in instances where there are few non-zero streamflows. We do this by encouraging the d parameter in the bias-correction (Eq. 3) to go to zero. That is, we encourage the error model to discount information from the forecast and to return a climatology ($z_2 \approx \mu$). This is achieved by placing a prior on the d parameter:

$$d \sim N(0, \sigma_d^2). \quad (11)$$

where the standard deviation, σ_d , controls the strength of the prior: smaller values encourage d to take values closer to zero. We test the values $\sigma_d = 0.25, 0.5, 1.0, 2.0, 4.0$. Because of the use of the prior, this estimation approach is no longer formally MLE, but a *maximum a posteriori* (MAP) estimation. The posterior density used to estimate the parameters is given in Appendix C (Equation C.3).



4 Results and discussion

4.1 Continent-wide performance of the base FoGSS model

Analysis of bias and statistical analysis of all 63 catchments will be described in the results of the three experiments we have conducted, below. We illustrate the overall performance of the FoGSS base case by reviewing skill and reliability for the six case study catchments.

In general, FoGSS performs well in perennial catchments, and this is reflected in the Herbert, Goobarragandra and Ringarooma rivers, shown in Figure 3. Forecasts are generally skillful at shorter lead times (typically <3 months), and thereafter become neutrally skillful. In some perennial catchments, forecasts can be strongly skillful to long lead times (e.g. 6 months or more in the Goobarragandra River), while catchments with little catchment memory (e.g. Ringarooma River) may only be skillful to lead-0 (i.e., in the first month). Regardless of the level of skill, we consider FoGSS to perform its role adequately when it does not return negatively skillful forecasts for any month or lead time. Some moderately negative skills do occur in the Herbert catchment, in low-flow months at longer lead times (e.g. August), because slight mispredictions of flow issued in wetter months (e.g. February) can result in proportionally larger errors in drier months at longer lead times. FoGSS also performs well in the ephemeral Fitzroy catchment, returning either positive or neutral skill for all months and lead times.

In more strongly ephemeral catchments, performance can be poor. In the seasonally ephemeral Eppalock catchment, forecast skill is strongly negative in the dry months from January to April, although the forecasts perform well at other times of the year. In the Ranken catchment, which experiences high incidences of zero flows year-round, performance is poor for a majority of months and lead times.

The cause of the poor forecast skill in the Ranken and Eppalock catchments is evident when we consider PIT plots (Figure 4). Forecasts are highly reliable for the perennial Herbert, Ringarooma and Goobarragandra catchments, as well as the Fitzroy catchment, for all months and lead times. Forecasts are not reliable for the dry months of the Eppalock (see February in Figure 3), and particularly unreliable for drier months in the Ranken catchment (e.g. September). The bowed shape of the PIT plots in Eppalock is evidence of a persistent bias – a tendency to overestimate flows – in the drier months, driven by an underestimation of the incidence of zero flows. The same problem exists in the Ranken catchment, but to a stronger degree. We have established in earlier work that post-processing rainfall forecasts with CBaM is able to produce highly reliable forecast rainfall ensembles (e.g., Peng et al., 2014; Schepen et al., 2012), meaning the problem lies with the hydrological error model. In catchments where more than half of streamflow observations are zero, FoGSS will always underestimate the incidence of zero flows. This is because the error model is assumed to follow a symmetrical distribution (Gaussian after transformation) about the value of the forecast. Even if the forecast is zero before the error model is applied, randomly drawing from a symmetrical distribution will yield ~50% of values greater than zero. We will see in the following experiments that this can have a particularly strong influence on bias.

4.2 Experiment 1: ESP forecasts

Figure 5 summarises how forecast skill varies with lead time for all 63 catchments with both forecast and historical rainfall forcings. As described above (Section 4.1), at very short lead times (e.g. lead-0) FoGSS forecasts generated with forecast rainfall are very often skillful. Skill at lead-0 is overwhelmingly positive in perennial catchments, but is generally also positive in ephemeral catchments. Skill subsides with lead time, with forecast skill in ephemeral catchments declining more rapidly. By lead-6, forecasts are generally neutrally skillful. Instances of strongly



negative skill ($< -15\%$) are rare in perennial catchments, and generally not present in longer lead times in ephemeral catchments. Strongly negative skills do occur in very dry catchments, as with the Ranken catchment described above.

5 Figure 5 shows that skill at individual lead times is generally not strongly influenced by changing the rainfall forcing to ESP. This generally highlights the predominant role catchment memory plays in generating skilful forecasts. Forecast rainfall tends to produce slightly more skilful forecasts at lead-3 and lead-6 in perennial catchments, but tends to produce more instances of negative skill at longer lead times (e.g. lead-9). Conversely, in ephemeral catchments historical rainfall forcings tend to be produce slightly more skilful streamflow forecasts than forecast rainfall forcings at all lead times.

10 Forecast rainfall shows slightly more evident benefits, however, when we consider forecasts of accumulated volumes. Figure 6 shows forecast skill calculated for forecasts of total streamflow volume accumulated over 1, 3, 6, 9 and 12 month periods. In ephemeral catchments, ESP forecasts are slightly better, with fewer instances of strongly negative skill, particularly for shorter accumulation volumes. In perennial catchments, however, forecast rainfall produces slightly, but noticeably, more skilful streamflow forecasts for accumulation periods of 6 months or more. We note that FoGSS forecasts for perennial catchments generally exhibit positive skill for accumulation periods up to 6 months, giving clear evidence of the information content of these forecasts over that of stochastic scenarios, irrespective of forcing.

Historical rainfall forcings do, however, have a clear advantage in reducing bias, particularly in ephemeral catchments (Figure 7). Bias is calculated using the mean of the forecast ensemble. Because the BJP models used to post-process POAMA make use of data transformation, the forecasts are unbiased in the transform domain. However, the back-transformation means that forecast ensemble means become separated from (and larger than) ensemble medians, resulting in positive biases. These positive biases are often slight ($\sim 5\%$), but can be amplified by the rainfall-runoff model. This amplification is particularly prevalent in ephemeral catchments, where the responses of runoff to rainfall can be highly non-linear. We note, however, that even with historical rainfall forcings, streamflow forecasts can be heavily biased. In very dry catchments this is partly due to the underestimation of the incidence of zero flows, as described in Section 4.1, above.

25 Streamflow forecasts generated from historical rainfall forcings show similar reliability to those generated with forecast rainfall forcings (not shown for brevity).

4.3 Experiment 2: hydrological modelling

30 Figures 8 and 9 show how forecast skill and bias vary with the choice of rainfall-runoff model. In general, the skill is similar for all three models, but both GR2M and Wapaba are noticeably less biased than ABCD. Wapaba and GR2M are similarly skilful and exhibit similar biases in perennial catchments. GR2M moderates some of the very negative skill scores and high catchment biases produced by Wapaba in very dry ephemeral catchments, which suggests that Wapaba's infinite groundwater store is not well suited to ephemeral rivers. Like many models, Wapaba can underestimate flows in wet seasons by pushing too much water into groundwater stores and diverting too little through direct runoff. These underestimations have little impact on forecast skill in high flow months. However, the excess water that is pushed into the infinite groundwater store cannot be lost, so it eventually drains out in dry seasons. This can result in substantial overestimation of streamflow in very dry seasons, which causes high proportional errors and biases. While we apply a bias-correction in the error model, Wapaba's overestimation



in dry months is caused by isolated (i.e., rare) events, which are difficult to capture under cross-validation. GR2M's ability to destroy water held in its groundwater store appears to be important for accounting for the high losses that can occur in drylands. GR2M requires the error model to do less work, making the system less prone to errors/bias under cross-validation in ephemeral rivers. Despite the benefits of GR2M over Wapaba, we note that Wapaba's Budyko-based structure remains theoretically attractive. We plan to explore ways to improve Wapaba's simulation of ephemeral rivers in future research.

A noteworthy finding of this experiment is that the choice of rainfall-runoff model did not have a major impact on forecast skill in perennial catchments. While a considerable amount of effort is often expended on selecting rainfall-runoff models for particular purposes, our results suggest that, at least at the monthly time step, a well-designed error model can mitigate various deficiencies in rainfall-runoff models for wide-scale application to perennial rivers.

4.4 Experiment 3: encouraging error model to return climatology forecasts

As we expect, the application of a prior on the σ_d parameter has negligible effect on the skill of forecasts in perennial rivers at all lead times (Figure 10). However, applying the prior did reduce some of the strongly negative skills experienced in ephemeral catchments at all lead times. The stronger the prior, the more that negative skills were removed, with the effect of the prior becoming negligible for $\sigma_d \geq 2.0$. Similarly, bias is greatly reduced by applying a strong prior to ephemeral rivers (Figure 11), as the forecasts have a reduced tendency to overestimate flows in very dry months. Interestingly, applying a strong prior also reduced biases in perennial catchments. This indicates that the prior is guarding against over-fitting of the bias-correction in these instances, with virtually no reduction in positive forecast skill. The reduction in bias has a slight positive impact on reliability in ephemeral rivers at longer lead times, as shown by the alpha index in Figure 12. However, the prior is unable to address the fundamental inability of FoGSS to generate a sufficient number zero flows in months where more than half of observed flows are zero, as discussed in Section 4.5.

In summary, the prior encourages FoGSS to behave sensibly. As already noted, strongly negative skills generally only occur in very dry months, where there may be only a few non-zero observations on which to optimise the hydrological and error models. In these cases, it is sensible to encourage FoGSS to return a climatology-like forecast. Conversely, when there are sufficient data to inform the optimisation of the models and the models perform well, the system should use the models. Using a prior in a MAP optimization enforces this sensible behavior in the model.

4.5 Synthesis

In each experiment, variations on the base case resulted in changes in forecast performance. The use of historical rainfall forcings is the least beneficial of the changes. Historical rainfall forcings can reduce bias, and this leads to fewer strongly negative skills, largely in very dry months and catchments. We note, however, the use of a strong prior has a stronger ability to remove bias in dry months than historical forcings (not shown), thus nullifying the benefits of the historical forcing. The use of historical forcings comes at the cost of removing information available from climate forecasts. We have shown that skill from climate forecasts can accumulate to produce skillful long-range total inflow forecasts. In addition, the POAMA model is being upgraded to a much higher resolution climate forecasting system by the Bureau of Meteorology (ACCESS-S), and this should result in stronger skill. On balance,



the inclusion of climate forecasts is beneficial, both for the additional skill available in some months/catchments with post-processed POAMA forecasts, but also for the prospect of including better climate forecasts in future.

To show the effects of the other variations, we combine forecast rainfall forcings with the GR2M model and a strong prior on d ($\sigma_d = 0.25$), and show forecast skill for our six example catchments in Figure 13. There are

5 some key differences between Figure 13 and forecast skill of the base case (Figure 3). In the very dry Ranken catchment, negative skill in wetter months (Jan-Apr) is largely removed, in favour of climatology-like forecasts. Conversely, skill in Jun, Aug and Dec has changed from neutral/positive in the base case to be substantially negative. In the Eppalock catchment, the variations on the base case have an unequivocal benefit: negative skill in the dry months of Jan-Apr is completely removed. In the other five catchments, the changes generally either

10 improve or have little impact on base case forecasts. There is little change to skill in the Fitzroy catchment, negative skill in the Herbert catchment in August is largely eliminated, and there are no discernible differences in skill in the Ringarooma and Goobarragandra catchments.

As already noted, the GR2M model's main benefit is in ephemeral catchments. In our example catchments in Figure 13, GR2M acts mainly to reduce negative skills in the Eppalock catchment in Feb and Mar by reducing

15 bias, with little differences in other catchments. As with the benefits of historical rainfall forcings, however, the ability of GR2M to reduce bias is largely subsumed by the use of a strong prior on the d parameter: similar reductions in negative skill in Eppalock are achieved when a prior on d is applied with the Wapaba model (not shown).

The use of a strong prior on d results in neutral to positive impacts on skill in most cases shown in Figure 13. The

20 exception is the very dry Ranken catchment, where the benefits of the prior are equivocal. The prior removes the base case's negative skills in the Ranken catchment in Jan-Mar, but also introduces negative skill in the drier months of Jun, Aug and Dec. We note that this may have practical benefits: in another study (Turner et al., 2017, this issue), we show that FoGSS forecasts can benefit reservoir operations in cases where forecasts are not skillful in very dry months, but positively or neutrally skillful at other times of the year. This is because the dry months

25 contribute little to the annual inflow volume, so small positive bias in dry months (the cause of negative skill) does not have a strong influence on the value of forecast. Conversely, a strong prior is responsible for removing negative skill in August in the Herbert catchment, and also removes the strongly negative skills in the Eppalock catchment in Jan-Apr. At the same time, the prior has little effect on the good performance of the base case in the Fitzroy, Ringarooma and Goobarragandra catchments.

30 We reiterate that the prior does not correct reliability problems in dry catchments, with PIT plots giving almost identical results to the base case (not shown for brevity). To mitigate the inherent tendency of the FoGSS error model to underestimate the occurrence of zero flows, we need to change its fundamental function. One approach for doing this would be to censor both simulations and observations in the MLE, and carry this approach through to generating forecasts. This would effectively change the assumption of a symmetrical error distribution about

35 forecasts of zero, and offset the error distribution to increase the incidence of zeros. We will explore this approach in future research.



5 Summary

We assess a new seasonal streamflow forecasting system called Forecast Guided Stochastic Scenarios (FoGSS) for continent-wide application in Australia. FoGSS uses post-processed climate model forecasts to force a monthly rainfall-runoff model, and applies a staged error model to quantify and propagate hydrological model uncertainty.

5 FoGSS is intended to provide a skillful alternative to resampled inflows for water agencies to use in operational planning: it is designed to extract skill from climate and catchment conditions, to produce unbiased and reliable ensemble predictions to 12 month forecast horizons, and to produce ‘coherent forecasts’ when forecast skill is not available – that is, forecasts that are similarly skillful to climatology. FoGSS is assessed on 63 Australian catchments, of which 21 are ephemeral rivers. FoGSS performs well in all but the driest catchments. Skill is generally positive at shorter lead times in both perennial and ephemeral catchments, and transits to neutral (zero) skill with respect to climatology at longer lead times. Forecast ensembles are generally reliable. However, in very dry catchments forecasts can be strongly negatively skillful and biased, in many cases because the ensembles are not reliable.

We conduct 3 experiments to establish whether components of the FoGSS system can be improved:

- 15 1. We use historical rainfall forcings – similar to ESP forecasts - to assess the contribution of forecast rainfall forcings to forecast skill
2. We assess three monthly rainfall-runoff models (Wapaba, GR2M, ABCD)
3. We use a Bayesian prior in our parameter estimation procedure to encourage the FoGSS error model to return climatology forecasts in months where the hydrological model performs poorly

20 Historical rainfall forcings sometimes improve forecasts (largely in very dry catchments) by reducing bias. However, this comes at the cost of including useful information in rainfall forecasts. On balance we believe the inclusion of seasonal rainfall forecasts in the FoGSS system is beneficial.

Wapaba and GR2M clearly outperform the ABCD rainfall-runoff model, and GR2M performs slightly better than Wapaba in ephemeral catchments. However, the advantages of the GR2M model are overshadowed by the use of the Bayesian prior. The prior reduces the instances of negative forecast skill and reduces bias in ephemeral catchments, and has little effect on performance in perennial catchments. The use of the prior does not, however, result in reliable forecast ensembles in catchments where zero flows occur more than half the time. We point to future research that could improve reliability in these very dry catchments.

6 Acknowledgements

30 This research has been supported by the Water Information Research and Development Alliance (WIRADA) between the Bureau of Meteorology and CSIRO Land & Water. Thanks to Senlin Zhou, Julien Lerat, Paul Feikema and Daehyok Shin (all Bureau of Meteorology) for supplying data and for fruitful discussions on the development of FoGSS.

References

35 Alley, W. M.: On the Treatment of Evapotranspiration, Soil Moisture Accounting, and Aquifer Recharge in Monthly Water Balance Models, *Water Resources Research*, 20, 1137-1149, doi:10.1029/WR020i008p01137, 1984.



-
- Beckers, J. V. L., Weerts, A. H., Tjeldeman, E., and Welles, E.: ENSO-conditioned weather resampling method for seasonal ensemble streamflow prediction, *Hydrol. Earth Syst. Sci.*, 20, 3277–3287, doi:10.5194/hess-20-3277-2016, 2016.
- Bell, V. A., Davies, H. N., Kay, A. L., Brookshaw, A., and Scaife, A. A.: A national-scale seasonal hydrological forecast system: development and evaluation over Britain, *Hydrol. Earth Syst. Sci. Discuss.*, 2017, 1–19, doi:10.5194/hess-2017-154, 2017.
- Bennett, J. C., Wang, Q. J., Li, M., Robertson, D. E., and Schepen, A.: Reliable long-range ensemble streamflow forecasts: Combining calibrated climate forecasts with a conceptual runoff model and a staged error model, *Water Resources Research*, 52, 8238–8259, doi:10.1002/2016wr019193, 2016.
- 10 Candogan Yossef, N., van Beek, R., Weerts, A., Winsemius, H., and Bierkens, M. F. P.: Skill of a global forecasting system in seasonal ensemble streamflow prediction, *Hydrol. Earth Syst. Sci. Discuss.*, 2016, 1–39, doi:10.5194/hess-2016-521, 2016.
- Clark, M. P., Gangopadhyay, S., Hay, L., Rajagopalan, B., and Wilby, R.: The Schaake shuffle: a method for reconstructing space–time variability in forecasted precipitation and temperature fields, *Journal of Hydrometeorology*, 5, 243–262, doi:10.1175/1525-7541(2004)005<0243:TSSAMF>2.0.CO;2, 2004.
- 15 Crochemore, L., Ramos, M. H., and Pappenberger, F.: Bias correcting precipitation forecasts to improve the skill of seasonal streamflow forecasts, *Hydrology and Earth System Sciences*, 20, 3601–3618, doi:10.5194/hess-2016-78, 2016.
- Day, G. N.: Extended streamflow forecasting using NWSRFS, *Journal of Water Resources Planning and Management*, 111, 157–170, doi:10.1061/(ASCE)0733-9496(1985)111:2(157), 1985.
- Del Giudice, D., Honti, M., Scheidegger, A., Albert, C., Reichert, P., and Rieckermann, J.: Improving uncertainty estimation in urban hydrological modeling by statistically describing bias, *Hydrology and Earth System Sciences*, 17, 4209–4225, doi:10.5194/hess-17-4209-2013, 2013.
- Gneiting, T., and Katzfuss, M.: Probabilistic forecasting, *Annual Review of Statistics and Its Application*, 1, 125–151, doi:10.1146/annurev-statistics-062713-085831, 2014.
- 25 Greuell, W., Franssen, W. H. P., Biemans, H., and Hutjes, R. W. A.: Seasonal streamflow forecasts for Europe – I. Hindcast verification with pseudo- and real observations, *Hydrol. Earth Syst. Sci. Discuss.*, 2016, 1–18, doi:10.5194/hess-2016-603, 2016.
- Hawthorne, S., Wang, Q. J., Schepen, A., and Robertson, D. E.: Effective use of GCM outputs for forecasting monthly rainfalls to long lead times, *Water Resources Research*, 49, 5427–5436, doi:10.1002/wrcr.20453, 2013.
- 30 Hudson, D., Marshall, A. G., Yin, Y., Alves, O., and Hendon, H. H.: Improving intraseasonal prediction with a new ensemble generation strategy, *Monthly Weather Review*, 141, 4429–4449, doi:10.1175/mwr-d-13-00059.1, 2013.
- Li, M., Wang, Q. J., and Bennett, J.: Accounting for seasonal dependence in hydrological model errors and prediction uncertainty, *Water Resources Research*, 49, 5913–5929, doi:10.1002/wrcr.20445, 2013.
- 35 Li, M., Wang, Q. J., Bennett, J. C., and Robertson, D. E.: A strategy to overcome adverse effects of autoregressive updating of streamflow forecasts, *Hydrology and Earth System Sciences*, 19, 1–15, doi:10.5194/hess-19-1-2015, 2015.



-
- Marshall, A. G., Hudson, D., Wheeler, M. C., Alves, O., Hendon, H. H., Pook, M. J., and Risbey, J. S.: Intra-seasonal drivers of extreme heat over Australia in observations and POAMA-2, *Climate Dynamics*, 43, 1915-1937, doi:10.1007/s00382-013-2016-1, 2014.
- Meißner, D., Klein, B., and Ionita, M.: Development of a monthly to seasonal forecast framework tailored to inland waterway transport in Central Europe, *Hydrol. Earth Syst. Sci. Discuss.*, 2017, 1-31, doi:10.5194/hess-2017-293, 2017.
- Mouelhi, S., Michel, C., Perrin, C., and Andréassian, V.: Stepwise development of a two-parameter monthly water balance model, *Journal of Hydrology*, 318, 200-214, doi:http://dx.doi.org/10.1016/j.jhydrol.2005.06.014, 2006.
- Peng, Z., Wang, Q. J., Bennett, J. C., Schepen, A., Pappenberger, F., Pokhrel, P., and Wang, Z.: Statistical calibration and bridging of ECMWF System4 outputs for forecasting seasonal precipitation over China, *Journal of Geophysical Research (Atmospheres)*, 119, 7116–7135, doi:10.1002/2013JD021162., 2014.
- Renard, B., Kavetski, D., Kuczera, G., Thyer, M., and Franks, S. W.: Understanding predictive uncertainty in hydrologic modeling: The challenge of identifying input and structural errors, *Water Resources Research*, 46, W05521, doi:10.1029/2009wr008328, 2010.
- Schaeffli, B., Talamba, D. B., and Musy, A.: Quantifying hydrological modeling errors through a mixture of normal distributions, *Journal of Hydrology*, 332, 303-315, doi:10.1016/j.jhydrol.2006.07.005, 2007.
- Schepen, A., Wang, Q. J., and Robertson, D. E.: Combining the strengths of statistical and dynamical modeling approaches for forecasting Australian seasonal rainfall, *Journal of Geophysical Research*, 117, D20107, doi:10.1029/2012JD018011, 2012.
- Schepen, A., and Wang, Q.: Ensemble forecasts of monthly catchment rainfall out to long lead times by post-processing coupled general circulation model output, *Journal of Hydrology*, 519, 2920–2931, doi:10.1016/j.jhydrol.2014.03.017, 2014.
- Schepen, A., Wang, Q. J., and Robertson, D. E.: Seasonal forecasts of Australian rainfall through calibration and bridging of coupled GCM outputs, *Monthly Weather Review*, 142, 1758-1770, doi:10.1175/mwr-d-13-00248.1, 2014.
- Schepen, A., Wang, Q. J., and Robertson, D. E.: Application to post-processing of meteorological seasonal forecasting, in: *Handbook of hydrometeorological ensemble forecasting*, 1 ed., edited by: Duan, Q., Pappenberger, F., Thielen, J., Wood, A., Cloke, H. L., and Schaake, J. C., Springer-Verlag Berlin Heidelberg, 1-29, 2016.
- Smith, T., Marshall, L., and Sharma, A.: Modeling residual hydrologic errors with Bayesian inference, *Journal of Hydrology*, 528, 29-37, doi:10.1016/j.jhydrol.2015.05.051, 2015.
- Thomas, H. A.: Improved methods for national water assessment, Harvard Water Resources Group, 1981.
- Turner, S. W. D., Bennett, J., Robertson, D., and Galelli, S.: Value of seasonal streamflow forecasts in emergency response reservoir management, *Hydrol. Earth Syst. Sci. Discuss.*, 2017, 1-26, doi:10.5194/hess-2016-691, 2017.
- Wang, Q. J., Pagano, T. C., Zhou, S. L., Hapuarachchi, H. A. P., Zhang, L., and Robertson, D. E.: Monthly versus daily water balance models in simulating monthly runoff, *Journal of Hydrology*, 404, 166-175, doi:10.1016/j.jhydrol.2011.04.027, 2011.
- Wang, Q. J., and Robertson, D. E.: Multisite probabilistic forecasting of seasonal flows for streams with zero value occurrences, *Water Resources Research*, 47, W02546, doi:10.1029/2010WR009333, 2011.



-
- Wang, Q. J., Schepen, A., and Robertson, D. E.: Merging seasonal rainfall forecasts from multiple statistical models through Bayesian model averaging, *Journal of Climate*, 25, 5524-5537, doi:10.1175/JCLI-D-11-00386.1, 2012a.
- Wang, Q. J., Shrestha, D. L., Robertson, D. E., and Pokhrel, P.: A log-sinh transformation for data normalization and variance stabilization, *Water Resources Research*, 48, W05514, doi:10.1029/2011WR010973., 2012b.
- 5 Wood, A. W., and Lettenmaier, D. P.: An ensemble approach for attribution of hydrologic prediction uncertainty, *Geophysical Research Letters*, 35, L14401, doi:10.1029/2008gl034648, 2008.
- Yuan, X.: An experimental seasonal hydrological forecasting system over the Yellow River basin – Part 2: The added value from climate forecast models, *Hydrology and Earth System Sciences*, 20, 2453-2466, doi:10.5194/hess-20-2453-2016, 2016.
- 10 Zhao, T., Schepen, A., and Wang, Q. J.: Ensemble forecasting of sub-seasonal to seasonal streamflow by a Bayesian joint probability modelling approach, *Journal of Hydrology*, 541, Part B, 839-849, doi:10.1016/j.jhydrol.2016.07.040, 2016.
- Zhao, T., Bennett, J. C., Wang, Q. J., Schepen, A., Wood, A. W., Robertson, D. E., and Ramos, M.-H.: How suitable is quantile mapping for post-processing GCM precipitation forecasts?, *Journal of Climate*, doi:10.1175/jcli-d-16-0652.1, 2017.
- 15



Tables

Table 1 Case study catchments

| Gauge Name | Gauge number | State | Perennial/ Ephemeral | Catchment area (km ²) | Longitude | Latitude | Missing data (%) |
|------------------------------------------|--------------|-------|-------------------------|-----------------------------------|-----------|----------|------------------|
| Goobarragandra River above Lacmalac | 410057 | NSW | Perennial | 668 | 148.35 | -35.33 | 0.3 |
| Ranken River at Soudan Homestead | G0010005 | NT | Ephemeral | 4,360 | 137.02 | -20.05 | 8.3 |
| Herbert River above Abergowrie | 116006B | QLD | Perennial | 7,486 | 145.92 | -18.49 | 0.0 |
| Ringarooma River at Moorina Bridge | 30 | TAS | Perennial | 517 | 147.87 | -41.13 | 8.0 |
| Lake Eppalock inflows (Campaspe River) | Inflows site | VIC | Ephemeral | 1,749 | 144.56 | -36.88 | 0.0 |
| Fitzroy River at Fitzroy Crossing Bridge | 802055 | WA | Ephemeral | 46,133 | 125.58 | -18.21 | 0.3 |



Figures

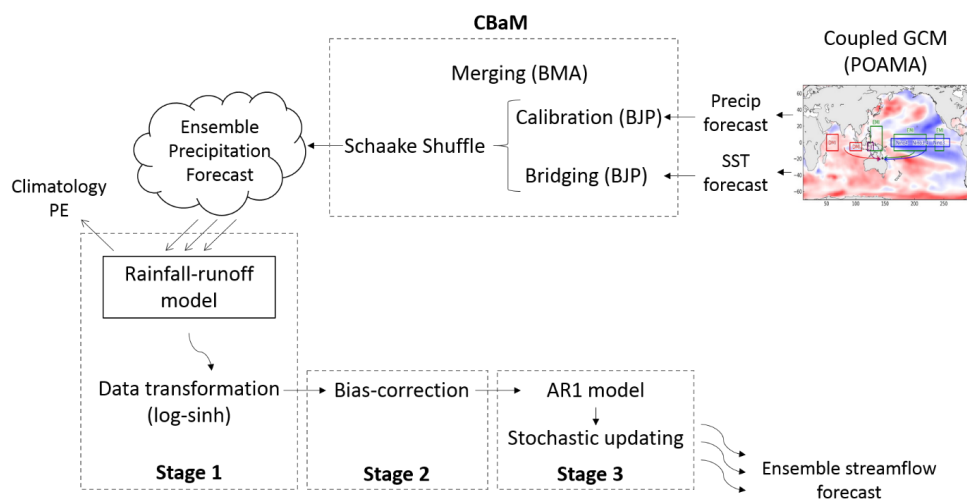


Figure 1: Schematic of the FoGSS model

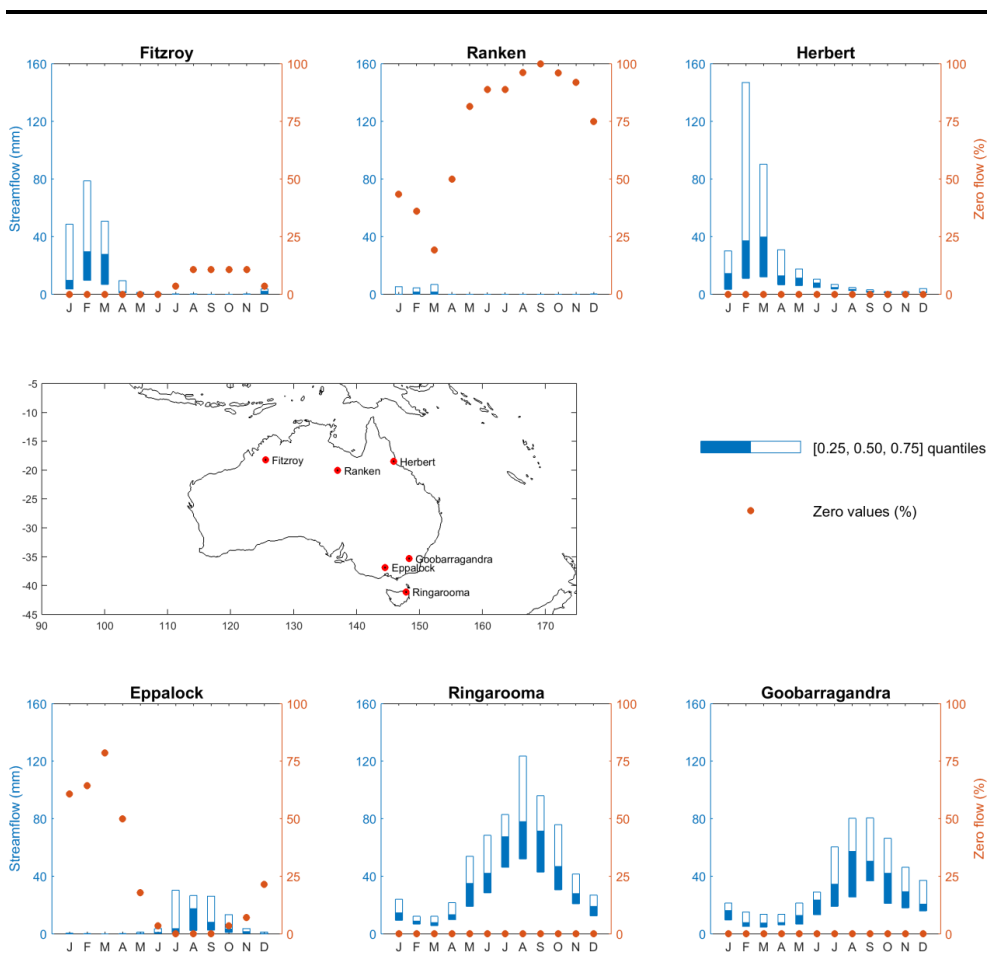


Figure 2: Catchment characteristics of six case study catchments. Left axis shows monthly streamflow characteristics, with blue bars showing interquartile range and median flows for the period 1982-2009. Right axis shows proportion of zero flows (orange points) in each month for the period 1982-2009.

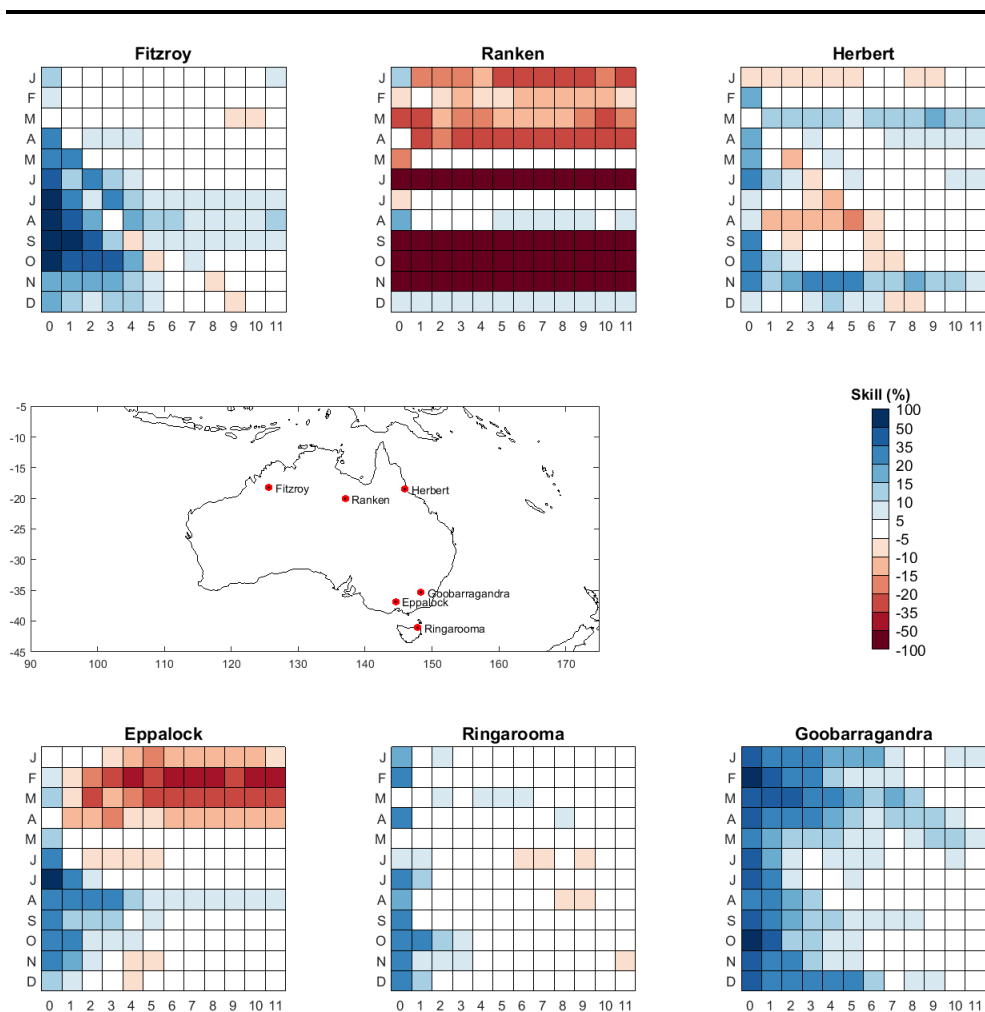


Figure 3: CRPS skill scores for FoGSS forecasts (base case). Target months are shown on the vertical axes, and target lead times on the horizontal axes. Centre map gives catchment locations.

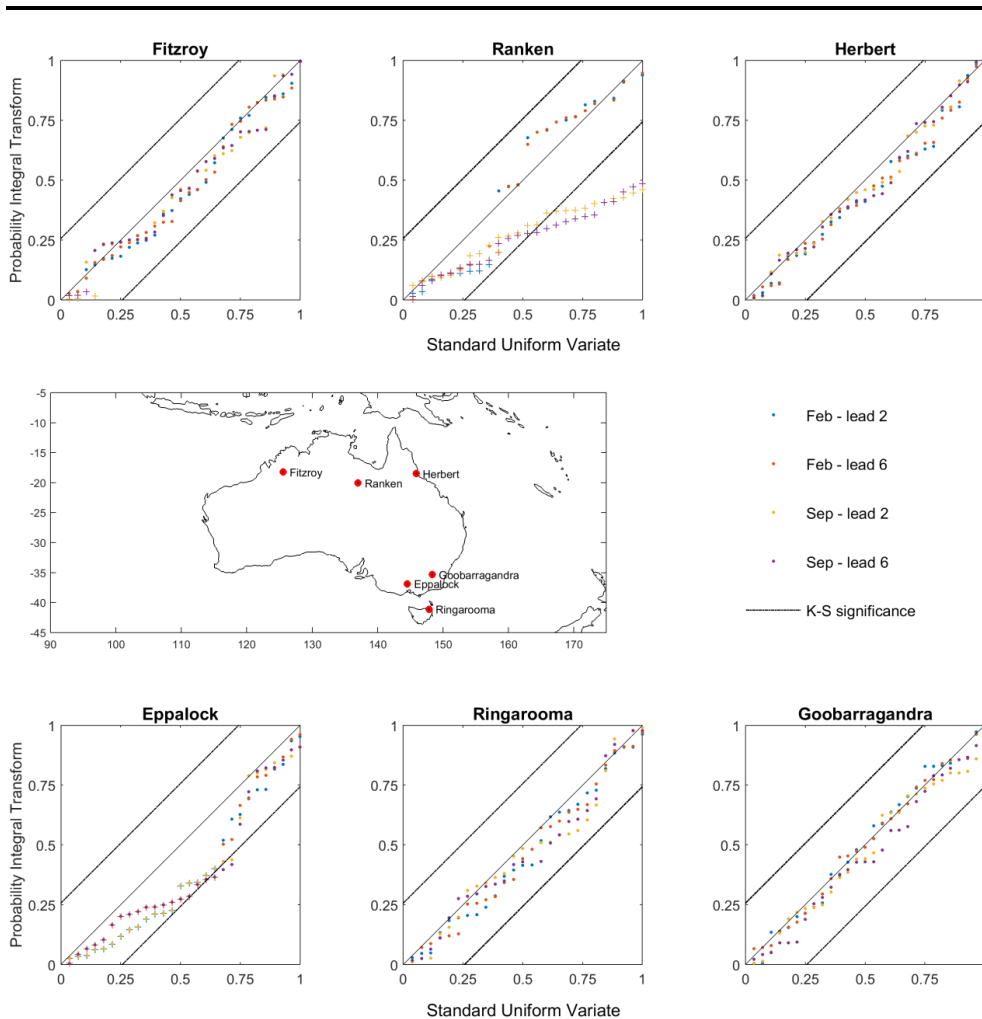
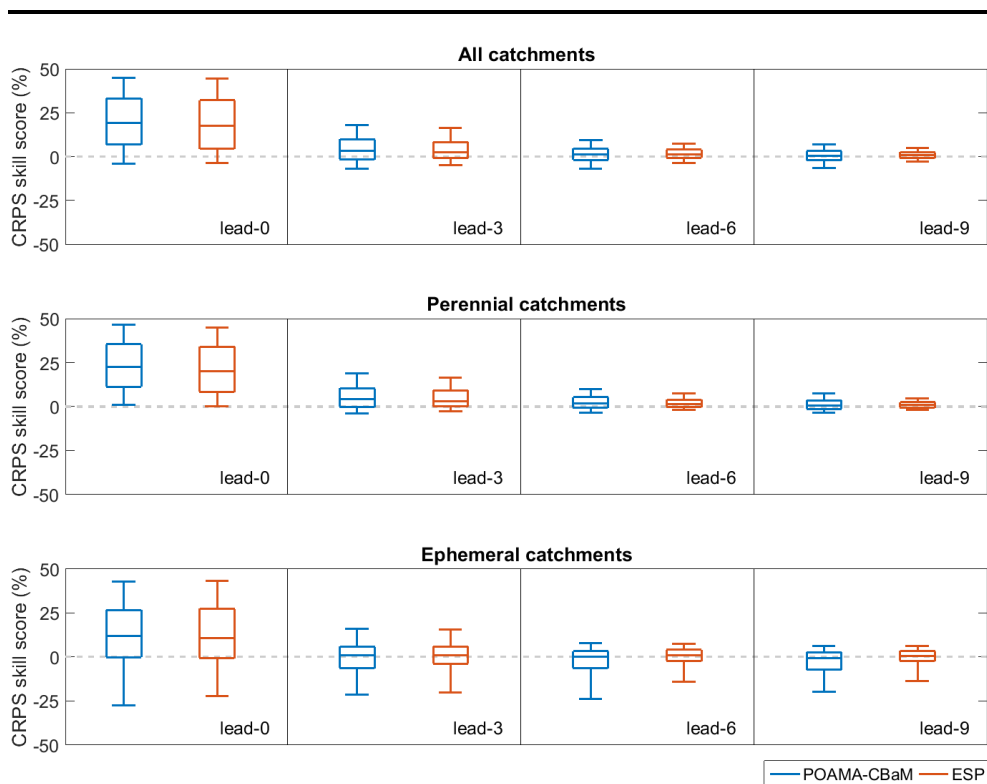
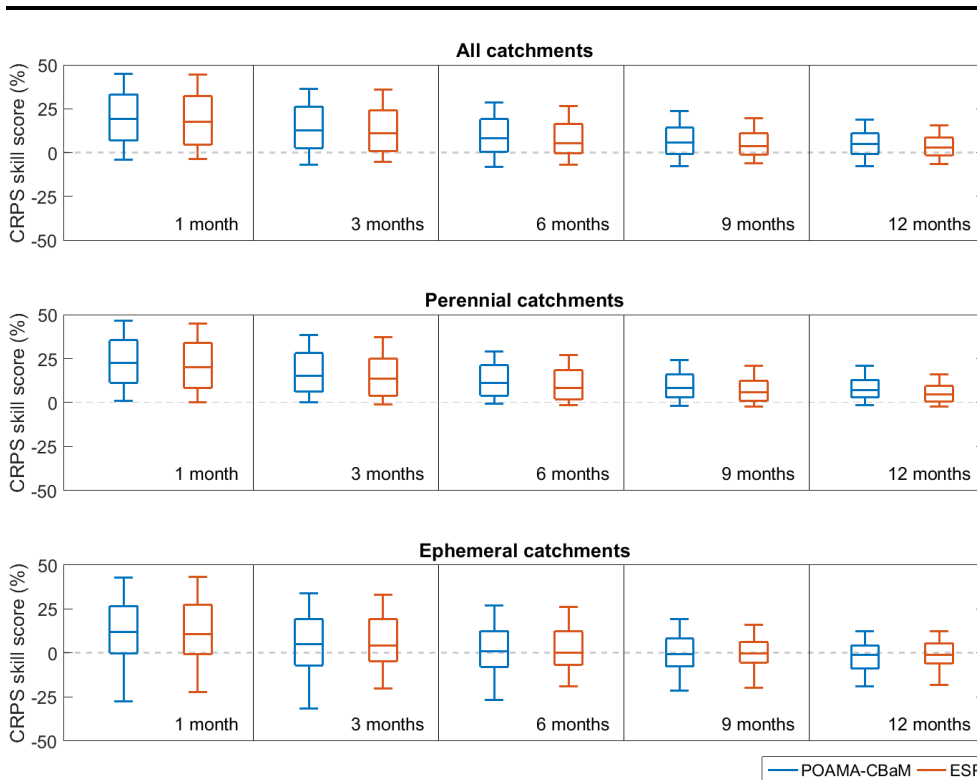


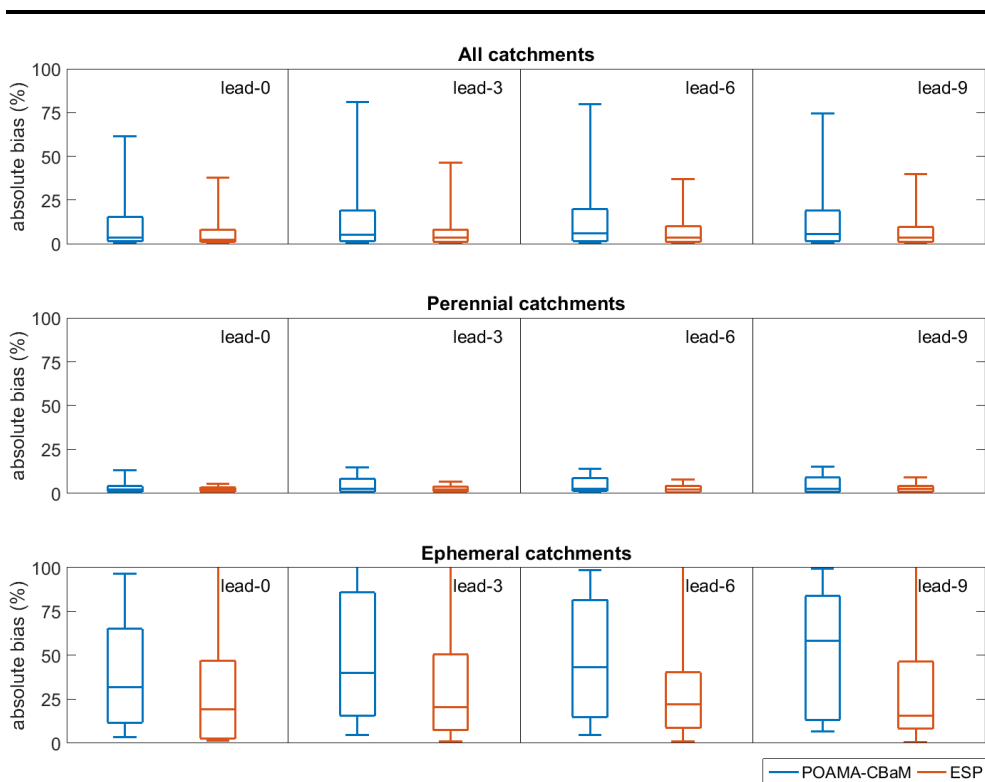
Figure 4: PIT plots for selected months and lead times (colours) for FoGSS forecasts (base case). Points are PIT values, crosses are pseudo-PIT values. Centre map gives catchment locations.



5 **Figure 5:** Forecast skill for all 63 catchments by lead time for FoGSS forecasts forced by forecast (POAMA-CBaM) and historical (ESP) rainfall. For each lead time, forecast skill is summarised for all months and catchments with box and whisker plots. Boxes show interquartile range with the median, whiskers give 10th and 90th percentiles. Top panel shows all catchments, middle panel shows perennial catchments, and bottom panel shows ephemeral catchments.



5 **Figure 6:** Forecast skill for 63 catchments by forecast accumulation period for FoGSS forecasts forced by forecast (POAMA-CBaM) and historical (ESP) rainfall. For each lead time, forecast skill is summarised for all months and catchments with box and whisker plots. Boxes show interquartile range with the median, whiskers give 10th and 90th percentiles. Top panel shows all catchments, middle panel shows perennial catchments, and bottom panel shows ephemeral catchments.



5 **Figure 7: Absolute bias in 63 catchments by lead time for FoGSS forecasts forced by forecast (POAMA-CBaM) and historical (ESP) rainfall. For each lead time, absolute bias is calculated for all months, and then summarised for all catchments with box and whisker plots. Boxes show interquartile range with the median, whiskers give 10th and 90th percentiles. Top panel shows all catchments, middle panel shows perennial catchments, and bottom panel shows ephemeral catchments.**

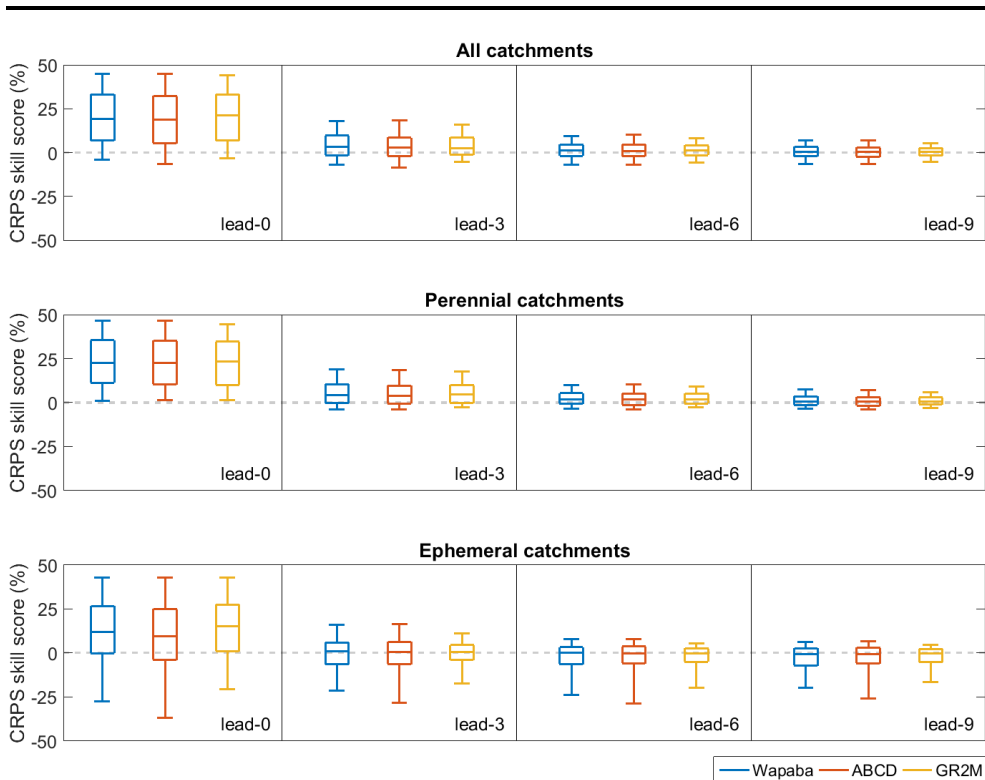


Figure 8: Forecast skill in 63 catchments by lead time for FoGSS forecasts with different rainfall-runoff models. For each lead time, forecast skill is summarised for all months with box and whisker plots. Boxes show interquartile range with the median, whiskers give 10th and 90th percentiles. Top panel shows all catchments, middle panel shows perennial catchments, and bottom panel shows ephemeral catchments.

5

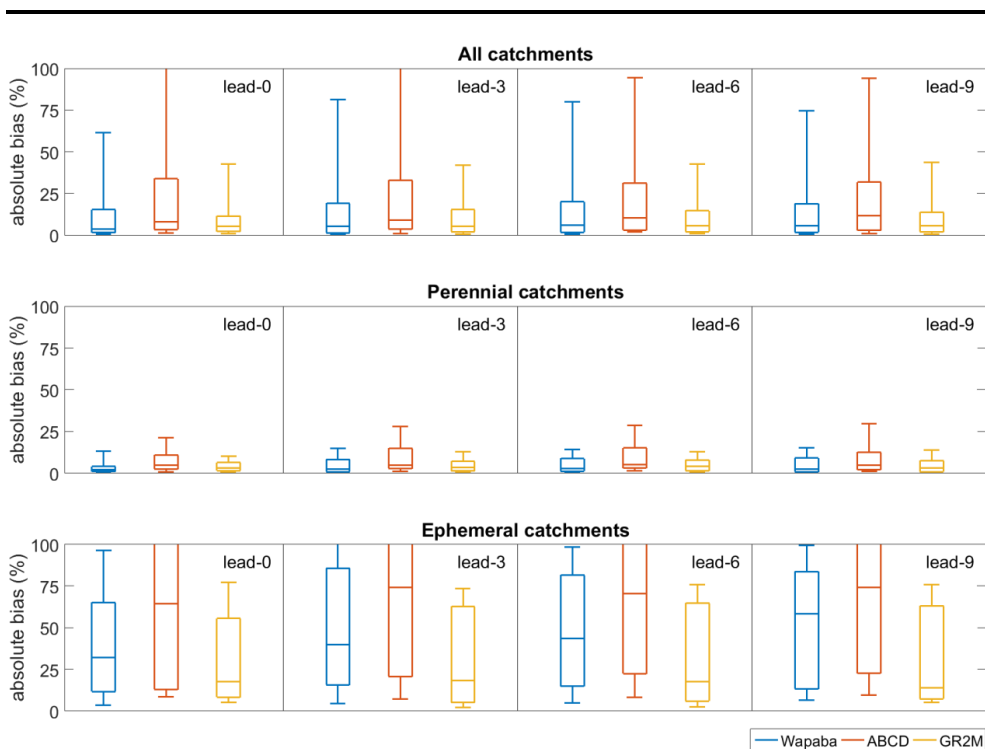


Figure 9 Absolute bias in 63 catchments by lead time for FoGSS forecasts with different rainfall-runoff models. For each lead time absolute bias is calculated for all months, and then summarised for all catchments with box and whisker plots. Boxes show interquartile range with the median, whiskers give 10th and 90th percentiles. Top panel shows all catchments, middle panel shows perennial catchments, and bottom panel shows ephemeral catchments.

5

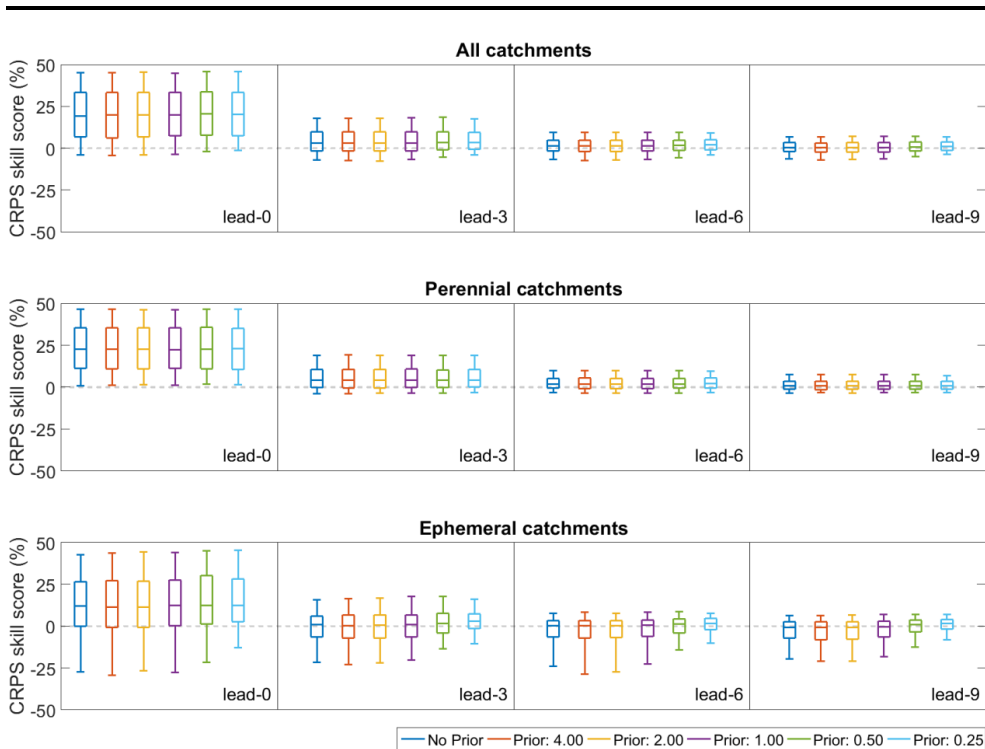
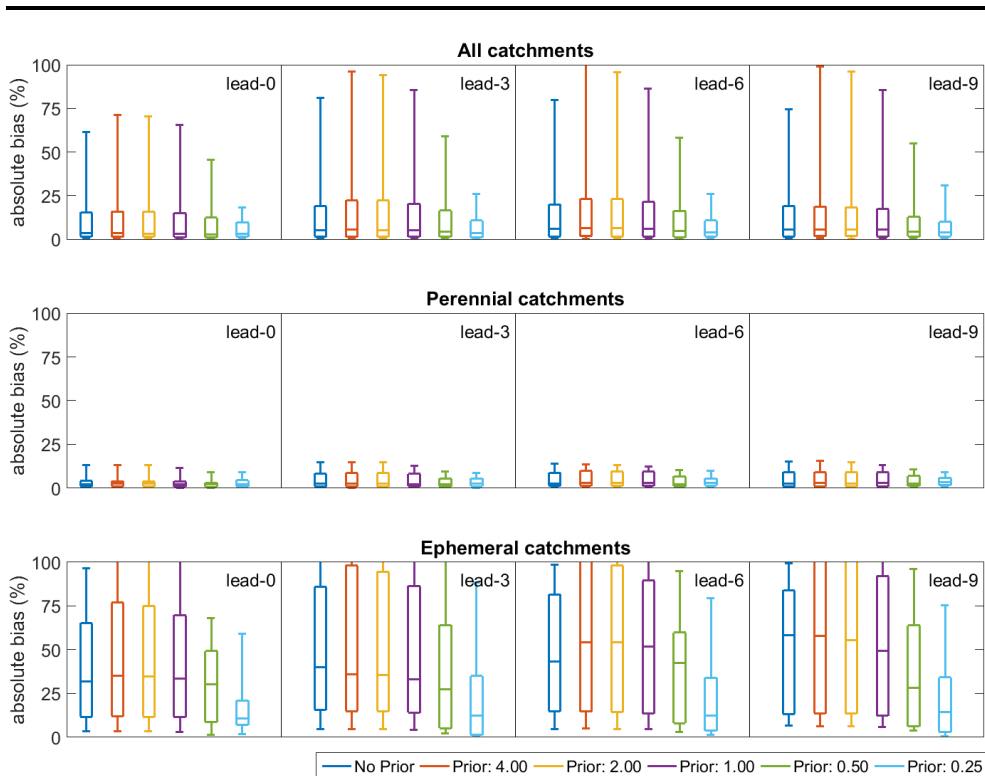


Figure 10: Forecast skill in 63 catchments by lead time for FoGSS forecasts with different strength priors on the d parameter. For each lead time, forecast skill is summarised for all months with box and whisker plots. Boxes show interquartile range with the median, whiskers give 10th and 90th percentiles. Top panel shows results for all catchments, middle panel for perennial catchments only, and bottom panel for ephemeral catchments.

5



5 **Figure 11:** Absolute bias in 63 catchments by lead time for FoGSS forecasts with different strength priors on the d parameter. For each lead time, forecast skill is summarised for all months with box and whisker plots. Boxes show interquartile range with the median, whiskers give 10th and 90th percentiles. Top panel shows results for all catchments, middle panel for perennial catchments only, and bottom panel for ephemeral catchments.

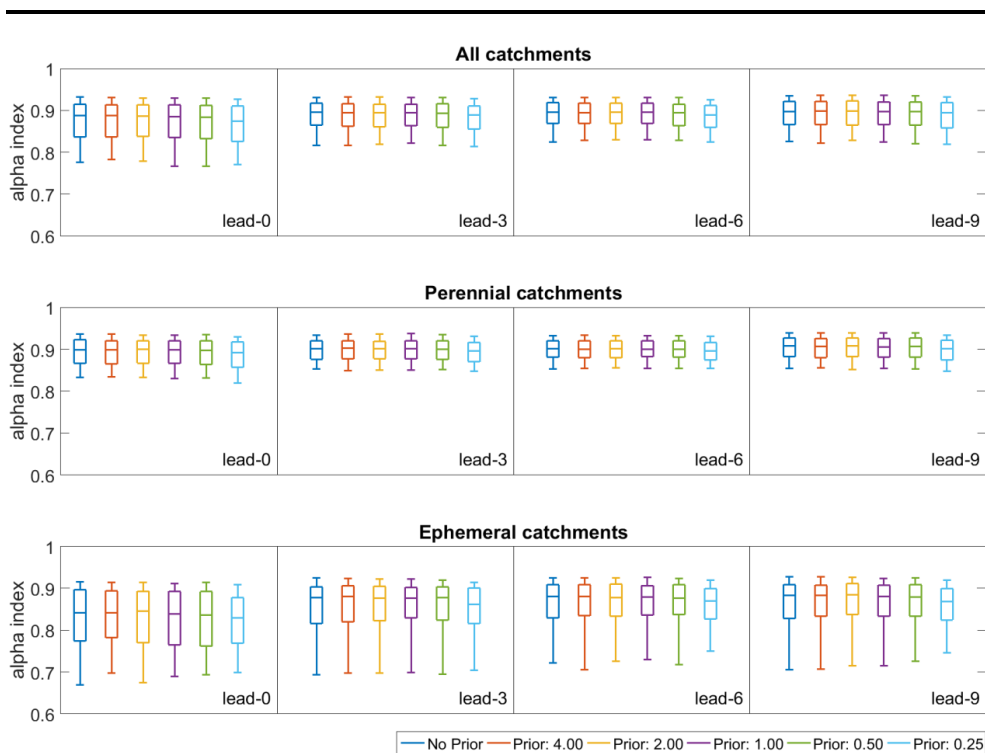


Figure 12: Reliability (alpha index) in 63 catchments by lead time for FoGSS forecasts with different strength priors on the d parameter. For each lead time, reliability is summarised for all months with box and whisker plots. Boxes show interquartile range with the median, whiskers give 10th and 90th percentiles. Top panel shows all catchments, middle panel shows perennial catchments, and bottom panel shows ephemeral catchments.

5

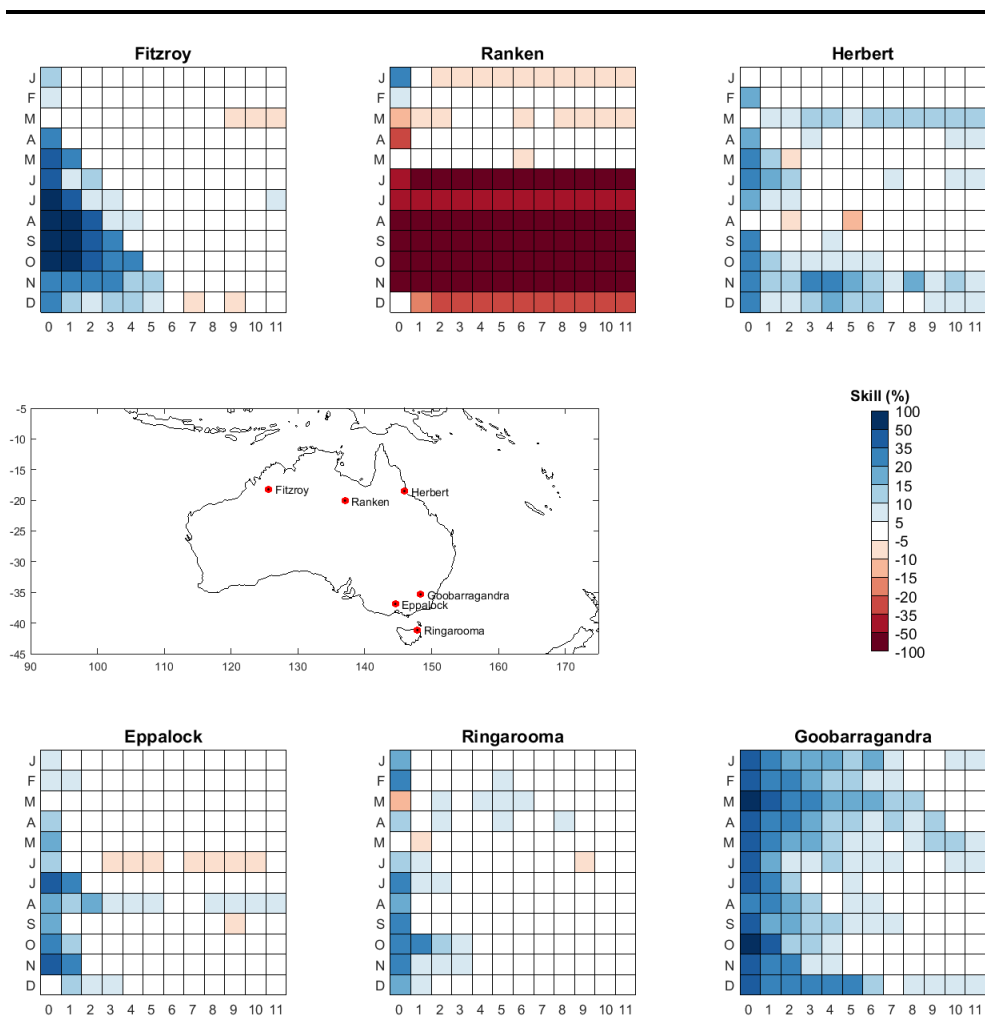


Figure 13: CRPS skill scores for FoGSS forecasts forced generated with the GR2M hydrological model and with a strong prior on the d parameter of $\sigma_d = 0.25$. Target months are shown on the vertical axes, and target lead times on the horizontal axes. Centre map gives catchment locations.

**Appendix A****Table A1: List of catchments**

| Gauge Name | Gauge number | State | Perennial/Ephemeral | Zero flows (%) | Area (km ²) | Lon | Lat | Missing data (%) |
|-------------------------------------------------|--------------|-------|---------------------|----------------|-------------------------|--------|--------|------------------|
| Abercrombie River above Hadley No.2 | 412066 | NSW | Perennial | 1.8 | 1631 | 149.6 | -34.11 | 2.7 |
| Burrinjuck Dam inflows | Inflows site | NSW | Perennial | 0.0 | 10,310 | 148.58 | -35.00 | 0.0 |
| Corang River at Hockeys | 215004 | NSW | Perennial | 0.9 | 166 | 150.03 | -35.15 | 4.2 |
| Cotter River above Gingera | 410730 | NSW | Perennial | 0.0 | 130 | 148.82 | -35.59 | 1.2 |
| Goobarragandra River above Lacmalac | 410057 | NSW | Perennial | 0.0 | 668 | 148.35 | -35.33 | 0.3 |
| Goodradigbee River above Wee Jasper (Kashmir) | 410024 | NSW | Perennial | 0.0 | 990 | 148.69 | -35.17 | 10.1 |
| Murray River above Biggara | 401012 | NSW | Perennial | 0.0 | 1,257 | 148.05 | -36.32 | 3.9 |
| Nowendoc River above Rocks Crossing | 208005 | NSW | Perennial | 0.0 | 1,893 | 152.08 | -31.78 | 1.8 |
| Paroo River at Willarra Crossing | 424002 | NSW | Ephemeral | 19.9 | 35,239 | 144.46 | -29.24 | 0.0 |
| Wollomombi River above Coninside | 206014 | NSW | Perennial | 0.0 | 377 | 152.03 | -30.48 | 3.0 |
| Daly River at Mount Nancar | G8140040 | NT | Perennial | 0.0 | 47,100 | 130.74 | -13.83 | 4.8 |
| Hugh River at South Road Crossing | G0050115 | NT | Ephemeral | 32.3 | 3,140 | 133.43 | -24.35 | 4.2 |
| Katherine River at Railway Bridge | G8140001 | NT | Perennial | 0.0 | 8,640 | 132.26 | -14.46 | 3.3 |
| Ranken River at Soudan Homestead | G0010005 | NT | Ephemeral | 72.4 | 4,360 | 137.02 | -20.05 | 8.3 |
| Roper River at Red Rock | G9030250 | NT | Perennial | 0.0 | 47,400 | 134.42 | -14.70 | 14.6 |
| South Alligator River at El Sherana | G8200045 | NT | Perennial | 0.0 | 1,300 | 132.52 | -13.53 | 7.7 |
| West Alligator River at Upstream Arnhem Highway | G8190001 | NT | Perennial | 0.0 | 316 | 132.17 | -12.79 | 3.9 |
| Barron River above Picnic Crossing | 110003A | QLD | Perennial | 0.0 | 239 | 145.54 | -17.26 | 0.0 |
| Burdekin River above Sellheim | 120002 | QLD | Perennial | 0.6 | 36,230 | 146.43 | -20.01 | 7.1 |
| Coen River above Coen Racecourse | 922101B | QLD | Ephemeral | 5.1 | 170 | 143.2 | -13.94 | 6.0 |
| Diamantina River at Birdsville | A0020101 | QLD | Ephemeral | 26.8 | 119,034 | 139.37 | -25.91 | 3.3 |
| Dulhunty River at Dougs Pad | 926002A | QLD | Perennial | 2.3 | 332 | 142.42 | -11.83 | 8.0 |
| Herbert River above Abergowrie | 116006B | QLD | Perennial | 0.0 | 7,486 | 145.92 | -18.49 | 0.0 |
| Namoi River above North Cuerindi | 419005 | QLD | Perennial | 0.0 | 2,532 | 150.78 | -30.68 | 1.5 |



| | | | | | | | | |
|----------------------------------------|--------------|-----|-----------|------|---------|--------|--------|------|
| Nogoa River at Craigmore | 130209A | QLD | Ephemeral | 21.3 | 13,876 | 147.76 | -23.88 | 13.4 |
| Richmond River above Wiangaree | 203005 | QLD | Perennial | 0.0 | 712 | 152.97 | -28.51 | 0.6 |
| Stuart River at Proston Rifle Range | 136304A | QLD | Ephemeral | 16.7 | 1,546 | 151.55 | -26.18 | 41.1 |
| Stanley River above Peachester | 143303A | QLD | Perennial | 0.0 | 102 | 152.84 | -26.84 | 0.6 |
| Cooper Creek at Cullyamurra Water Hole | A0030501 | SA | Ephemeral | 20.2 | 232,846 | 140.84 | -27.7 | 0.0 |
| Myponga US Dam and Road Bridge | A5020502 | SA | Perennial | 0.3 | 71 | 138.48 | -35.38 | 4.5 |
| North Para River at Penrice | A5050517 | SA | Ephemeral | 11.1 | 121 | 139.06 | -34.46 | 3.3 |
| Davey River above D/S Crossing Rv | 473 | TAS | Perennial | 0.0 | 698 | 145.95 | -43.14 | 0.9 |
| Florentine above Derwent | 304040 | TAS | Perennial | 0.0 | 445 | 146.5 | -42.44 | 0.0 |
| Hellyer River above Guilford Junction | 61 | TAS | Perennial | 0.0 | 101 | 145.67 | -41.42 | 0.3 |
| Leven River at Bannons Bridge | 314207 | TAS | Perennial | 0.0 | 499 | 146.09 | -41.25 | 1.8 |
| North Esk River at Ballroom | 318076 | TAS | Perennial | 0.0 | 363 | 147.38 | -41.49 | 0.9 |
| Ringarooma River at Moorina Bridge | 30 | TAS | Perennial | 0.0 | 517 | 147.87 | -41.13 | 8.0 |
| Swan River at the Grange | 302200 | TAS | Perennial | 0.0 | 448 | 148.08 | -42.05 | 7.4 |
| Avoca River at Amphitheatre | 408202 | VIC | Ephemeral | 9.5 | 83 | 143.4 | -37.18 | 0.0 |
| Lake Eildon | Inflows site | VIC | Perennial | 0.0 | 3,877 | 145.97 | -37.16 | 0.0 |
| Lake Eppalock | Inflows site | VIC | Ephemeral | 25.6 | 1,749 | 144.56 | -36.88 | 0.0 |
| Goulburn River above Dohertys | 405219 | VIC | Perennial | 0.0 | 700 | 146.13 | -37.33 | 4.5 |
| Grace Burn Creek | Inflows site | VIC | Perennial | 0.0 | 25 | 145.55 | -37.64 | 0.0 |
| Lake Hume | Inflows site | VIC | Perennial | 1.5 | 11,754 | 147.15 | -36.08 | 0.0 |
| Mosquito Creek above Struan | A2390519 | VIC | Ephemeral | 10.7 | 1,249 | 140.77 | -37.09 | 0.0 |
| Mitta Mitta River above Hinnomunjie | 401203 | VIC | Perennial | 0.0 | 1,518 | 147.61 | -36.95 | 4.5 |
| O'Shannassy Reservoir | Inflows site | VIC | Perennial | 0.0 | 127 | 145.81 | -37.68 | 0.0 |
| Ovens inflows | Inflows site | VIC | Perennial | 0.0 | 7,515 | 146.33 | -36.36 | 0.0 |
| Tanjil Junction inflows | 85266 | VIC | Perennial | 0.0 | 289 | 146.19 | -37.98 | 0.0 |
| Thomson Reservoir | Inflows site | VIC | Perennial | 0.0 | 487 | 146.37 | -37.79 | 0.0 |
| Tambo River above Swifts Creek | 223202 | VIC | Perennial | 0.0 | 899 | 147.72 | -37.26 | 3.9 |
| Upper Yarra Reservoir | Inflows site | VIC | Perennial | 0.0 | 337 | 145.92 | -37.68 | 0.0 |
| Watts River inflows | Inflows Site | VIC | Perennial | 0.0 | 104 | 145.55 | -37.64 | 0.0 |
| Darkin River at Pine Plantation | 616002 | WA | Ephemeral | 50.8 | 665 | 116.29 | -32.07 | 0.9 |
| Denmark River at Mt Lindesay | 603136 | WA | Perennial | 5.1 | 502 | 117.31 | -34.87 | 0.0 |



| | | | | | | | | |
|--------------------------------------|--------------|----|-----------|------|--------|--------|--------|-----|
| Deep River above Teds Pool | 606001 | WA | Ephemeral | 17.0 | 468 | 116.62 | -34.77 | 0.0 |
| Fitzroy River at Fitzroy Crossing Br | 802055 | WA | Ephemeral | 4.2 | 46,133 | 125.58 | -18.21 | 0.3 |
| Gascoyne River at Nine Mile Bridge | 704139 | WA | Ephemeral | 60.1 | 74,432 | 113.77 | -24.83 | 0.0 |
| Harvey River above Dingo Road | 613002 | WA | Perennial | 0.6 | 148 | 116.04 | -33.09 | 2.4 |
| Marillana Creek at Flat Rocks | 708001 | WA | Ephemeral | 29.8 | 1370 | 118.97 | -22.72 | 0.0 |
| Ord River at Old Ord Homestead | 809316 | WA | Ephemeral | 26.2 | 19,513 | 128.85 | -17.37 | 3.3 |
| Serpentine Reservoir | Inflows site | WA | Ephemeral | 7.1 | 664 | 116.10 | -32.4 | 0.0 |
| Young River at Neds Corner | 601001 | WA | Ephemeral | 42.6 | 1,893 | 121.14 | -33.71 | 0.0 |

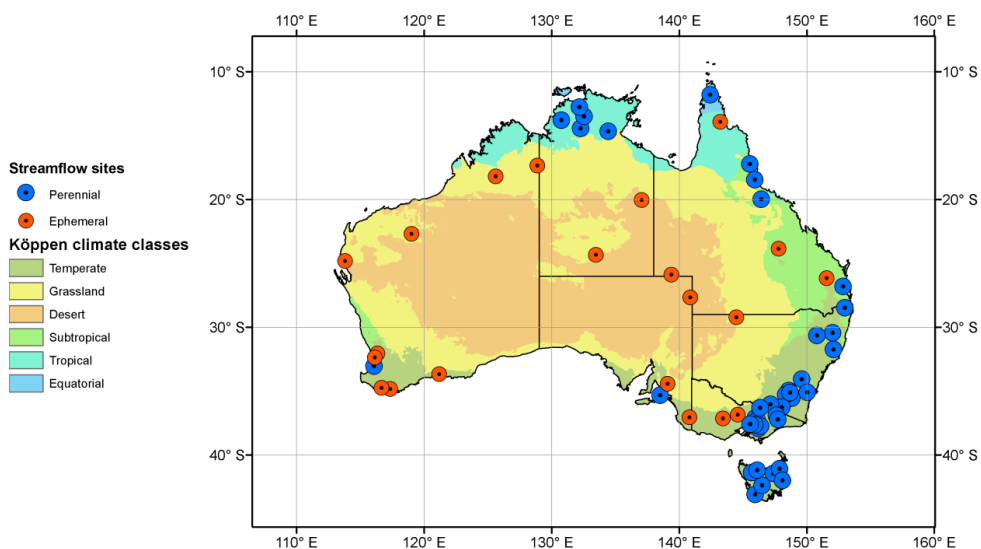


Figure A1: Distribution of gauge/inflows sites showing ephemeral/perennial streams



Appendix B

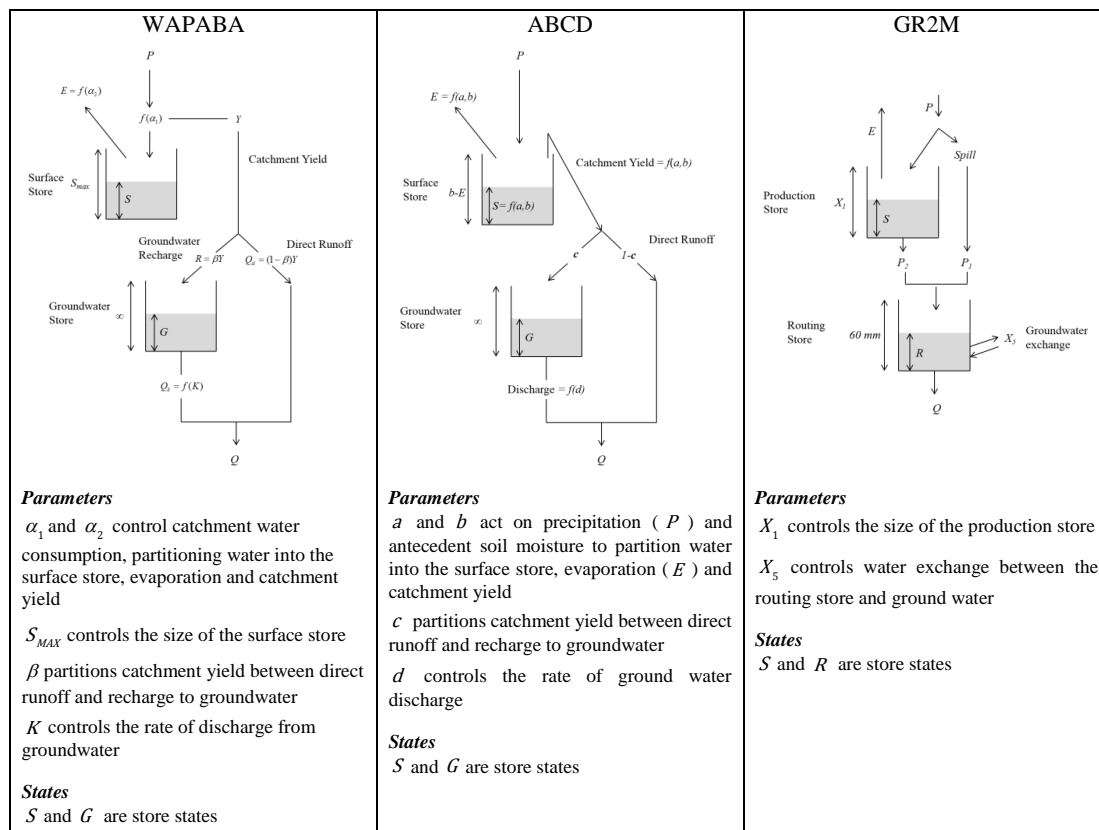


Figure B1: Hydrological model structures and parameters



Appendix C

C.1 Posterior density used for estimation of Stage 2 parameters

We assume that residuals are normally distributed. Because parameters in Eq. (3) vary by month it follows that the residual distribution also varies by month:

$$\begin{aligned} z_o(t) &= z_2(t) + \varepsilon_2(i) \\ \varepsilon_2(i) &\sim N(0, \sigma_2^2(i)) \end{aligned} \quad (C1)$$

The Stage 2 parameters to be estimated (from Eq. 3 and Eq. C1) are denoted as

$$\theta_2(i) = \{d(i), \mu(i), \sigma_2(i)\}. \quad (C2)$$

We maximize the posterior density

$$p(q_o(t) | \theta_2(i), q_1(t)) \propto p(d) \prod_{t \in \mathcal{T}_1} J_{q \rightarrow z} \mathcal{N}(z_o(t) | z_2(t), \sigma_2(i)), \quad (C3)$$

10 where q_1 is the simulation produced with Stage 1, the Jacobian, $J_{z \rightarrow q}$, is given by

$$J_{z \rightarrow q} = \frac{1}{\tanh(a + bq_o(t))} \quad (C4)$$

and $p(d)$ is the a prior on the d parameter (Section 3.5),

$$p(d) = d \sim N(0, \sigma_d^2). \quad (C5)$$

If $q_o(t) = 0$, then the likelihood term $J_{q \rightarrow z} \mathcal{N}(z_o(t) | z_2(t), \sigma_2(i))$ in Eq. (C3) is substituted with the normal cumulative

15 probability $\Phi\left(\frac{z_c - z_2(t)}{\sigma_2(i)}\right)$, where $z_c = TF(0)$ is the log-sinh transformed value of zero (see Eq. 1).